Fracture Detection and Structural Dip Analysis from Oil-Base Microresistivity Image Logs in a Horizontal Well: A Case Study from the Silurian Longmaxi Shale*

Gao-Cheng Wang[1], Zhao Zhang[1], Qin-Fei Li[1], Kai-Gui Yin[1], Yu-Feng Luo[1], Heng Zhang[1], and Da-Li Wang[2]

Search and Discovery Article #42278 (2018)**
Posted October 29, 2018

*Adapted from extended abstract prepared in conjunction with poster presentation given at AAPG 2018 AAPG Annual Convention and Exhibition, Salt Lake City, Utah, May 20-23, 2018
 DOI:10.1306/42278Wang2018

[1]PetroChina Zhejiang Oil Field Company, Hangzhou, Zhejiang, China (zhangc85@petrochina.com.cn)
[2]DCS, Schlumberger, Chengdu, China (DWang7@slb.com)

Abstract

A large amount of mud loss and the cluster design of hydraulic fracture stimulation in an oil-based mud horizontal well motivated running oil-base microresistivity image logs in a 1600 m horizontal section in the Silurian Longmaxi Shale. The image log interpretation reveals the distribution of natural fractures in the horizontal section and indicates that the horizontal section cuts through the structural fault identified from structural dip analysis. However, the total mud loss of 342 m^3 occurred near the natural fractures in the horizontal section. This suggests that the fractures could cause a large amount of the mud loss. The attributes of the fractures and the fault were used as important inputs for the cluster design of hydraulic fracture stimulation in the horizontal well.

A total of 325 fractures in the horizontal section were recognized from the oil-base microresistivity image logs. In the target layer of the pilot hole of the horizontal well, 19 cemented fractures were interpreted from electrical image logs. Core observations from the pilot well and vertical offset wells indicate that the fractures in the Longmaxi Shale are fully cemented fractures. Both the core and electrical image logs suggest that the 325 fractures observed on the oil-base microresistivity images could also be fully cemented fractures.

Fractures and minor faults are very common because of complex structural fault system in the Silurian Longmaxi Shale. However, it is impossible to detect the fractures and minor faults from conventional open hole logs and seismic data because of resolution limitations. Water-base electrical image logs, such as wireline image logs and logging-while-drilling (LWD) image logs, cannot be run in an oil-based mud borehole. Although the oil-base microresistivity image log was a good solution for fracture and fault detection in the Longmaxi Shale, it has its limitation in the distinction between open fracture and cemented fracture. Core observation and the geological background of the Longmaxi Shale are used to overcome this limitation.

The case study presents that the attributes of fractures are important not only for the cluster design of hydraulic fracture stimulation, but also for better understanding the distribution of fractures in the Longmaxi Shale. The horizontal section drills through more fractures than the pilot hole

because the horizontal section trajectory is perpendicular to the high-angle fracture strike. Regarding further deployment methods, the new-generation oil-base microresistivity image logs will be used to distinguish between open fracture and cemented fracture by inversion processing.

Introduction

The Longmaxi Shale is part of the Lower Silurian Longmaxi Formation, which is currently the main target for marine shale gas exploration and development in China. The Longmaxi Formation in the subsurface of Sichuan Basin was affected by multiple tectonic movements and a long period of erosion. The Longmaxi Formation is present only in certain parts of the Sichuan Basin. The wells in this paper are in the Zhaotong area, southern Sichuan Basin.

The complex structures in the Longmaxi Formation cause a risk of mud loss in vertical and horizontal wells. The mud loss events commonly occur near the faults and fractures in the area. The accumulated volume of oil-base mud loss was up to 918.05 m^3 in one horizontal well with a horizontal section length of 1600 m from the entry point to the endpoint. Accumulated volumes of 596.85 m^3 and 338.6 m^3 of oil-base mud loss occurred separately in two other horizontal wells of the same multiwell pad; the horizontal section lengths were 1000 m and 1290 m, respectively. However, the mud loss also occurred in wells where seismic data did not identify any faults and fractures. It is known that some of the faults and fractures cannot be identified from seismic data due to seismic resolution limitation.

The case study in this paper demonstrates fracture and fault detection from oil-base microresistivity image logs. The core observation analysis from the pilot well validates the possible size and type of the fractures from the image logs; it helps to better understand where possible mud loss occurs in the horizontal section. The paper also presents the new-generation oil-base microresistivity image logs in a new horizontal well, which provides the resistivity images with high borehole coverage and high resolution. Four horizontal wells have been planned to run the new-generation oil-base microresistivity image logs in the area.

Structure from Seismic Data

The horizontal section length was planned as 1500 m from the entry point (A) to the endpoint (B), and the pretarget displacement of the horizontal well is about 391 m. Figure 1 shows the well trajectory and structure information from surface seismic data. The seismic data indicate that the structure of the target layer is gentle, with an average 9° dip between A and B without fault and structural dip variation.

Several faults were identified from an ant-tracking time slice on the bottom of the Ordovician Wufeng Formation, which underlies the Silurian Longmaxi Formation (Figure 2). However, the horizontal section does not intersect these faults.

Fractures in Core

Based on the 930 m of core from the Longmaxi Formation from the 16 wells in the Zhaotong area, the fracture types are mainly high-angle fractures, low-angle shear fractures with slickolites, and root-shaped cracks caused by shear-slip displacements, as shown in Figure 3. Each of the fracture lengths on the cores is less than 0.5 m. The slickolites are mainly developed in the Ordovician Wufeng Formation underlying the Silurian Longmaxi Formation. Few slickolites occur in the Silurian Longmaxi Formation.

All of the different types of fractures in the cores are almost fully filled with calcite (i.e., calcite veins). Graptolites are also visible in core sections. The calcite veins have a close relationship with the total organic content (TOC) and the content of the carbonate in the source rock (Luo et al., 2015; Wang et al., 2005). The fractures, however, play an important role in high gas production (Guo and Zhang, 2014; Guo, 2014).

Fractures from Image Logs

The appearance of the fractures differs between the water-base electrical images and oil-base microresistivity images (Figure 4). However, the core observation from the 16 wells suggests that the fractures could be fully filled with calcite veins.

A total of 325 fractures in the horizontal section were recognized from the oil-base microresistivity image logs. In the target layer of the pilot well, 19 fractures were interpreted from the electrical image logs, as shown in Figure 5. It is clear that the horizontal section drills through more fractures than the pilot hole, because the horizontal section trajectory is perpendicular to approximately 80° of the high-angle fractures. The horizontal section trajectory direction is southeast, and the fractures strike northeast/southwest.

Structure from Image Logs

The structural dip interpretation presents the dip pattern changes along the well trajectory (as seen by the color pattern of green–blue–red–green in Figure 6). This suggests that a geological event could be responsible for the red-blue dip pattern change. The static images appear to show an abrupt change in lithofacies at a depth of x876 m. This suggests the presence of a fault.

In fact, the well trajectory was drilling down in the Longmaxi Formation until at the depth x876 m, and then drilled out of the target layer into the Ordovician Wufeng carbonate formation, and drilled back to the Longmaxi Formation again at the depth x973 m. The structural dip interpretation suggests that the fault was the main cause of the trajectory drilling out of the target layer.

Mud Loss Analysis

The mud loss mainly occurred in the interval from x400 m to x900 m. A mud loss of 37 m^3 occurred at the depth x400 m, which was caused by the fractures in zone 1 (Figure 7). Mud loss of 153 m^3 occurred at the depth x596 m, which was caused by the fractures in zone 2, and mud loss of 93 m^3 occurred at the depth x773 m, which was caused by the fractures in zone 3 and the main fault. In all, 342 m^3 mud loss occurred in the horizontal section, and 28 m^3 of mud returned after stopping the pump for 40 minutes.

The fractures and fault were also important consideration in the cluster design of hydraulic fracture stimulation in the horizontal section. The fracture zones should be treated separately in different clusters.

Figure 8 presents the new-generation oil-base microresistivity image logs in a new horizontal well, which provides the resistivity images with high borehole coverage and high resolution.

Conclusions

The oil-base microresistivity image logs provide a good solution in an oil-base mud horizontal well for fracture detection and structural interpretation, particularly for the mud loss analysis and the cluster design of hydraulic fracture stimulation in a horizontal well.

The fractures, even with the lengths of less than 0.5 m, can cause significant mud loss in the Longmaxi shale formation. This could be because a fracturing network can easily develop in the brittle shale of the Longmaxi Formation.

Acknowledgments

The authors thank PetroChina Zhejiang Oilfield Company for supporting the oil-base microresistivity image log data acquisition. We thank PetroChina Zhejiang Oilfield Company for permission to publish this paper and to share the knowledge we have gained. We also thank the experts from the Zhejiang Oilfield Company and Schlumberger for their helpful discussion and support.

References Cited

Guo, T.L., and Zhang, H.R., 2014, Formation and Enrichment Mode of Jiaoshiba Shale Gas Field, Sichuan Basin: Petroleum Exploration and Development, v. 41/1, p. 28-36.

Guo, X.S., 2014, Rules of Two-Factor Enrichment for Marine Shale Gas in Southern China - Understanding from the Longmaxi Formation Shale Gas in Sichuan Basin and Its Surrounding Area: Acta Geologica Sinica, v. 88/7, p. 1209-1218.

Luo, H.Y., W.H. Liu, W.C. Wang, M. Fan, and Y.H. Han, 2015, Discovery of the Mineralogical Evidence of the Thermochemical Sulfate Reduction in Black Shale: Bulletin of Mineralogy, Petrology, and Geochemistry, v. 34/2, p. 330-333.

Wang, G.M., Y.J. Ren, J.H. Zhong, Z.P. Ma, and Z.X. Jiang, 2005, Genetic Analysis on Lamellar Calcite Veins in Paleogene Black Shale of the Jiyang Depression: Acta Geologica Sinica, v. 79/6, p. 834-838.

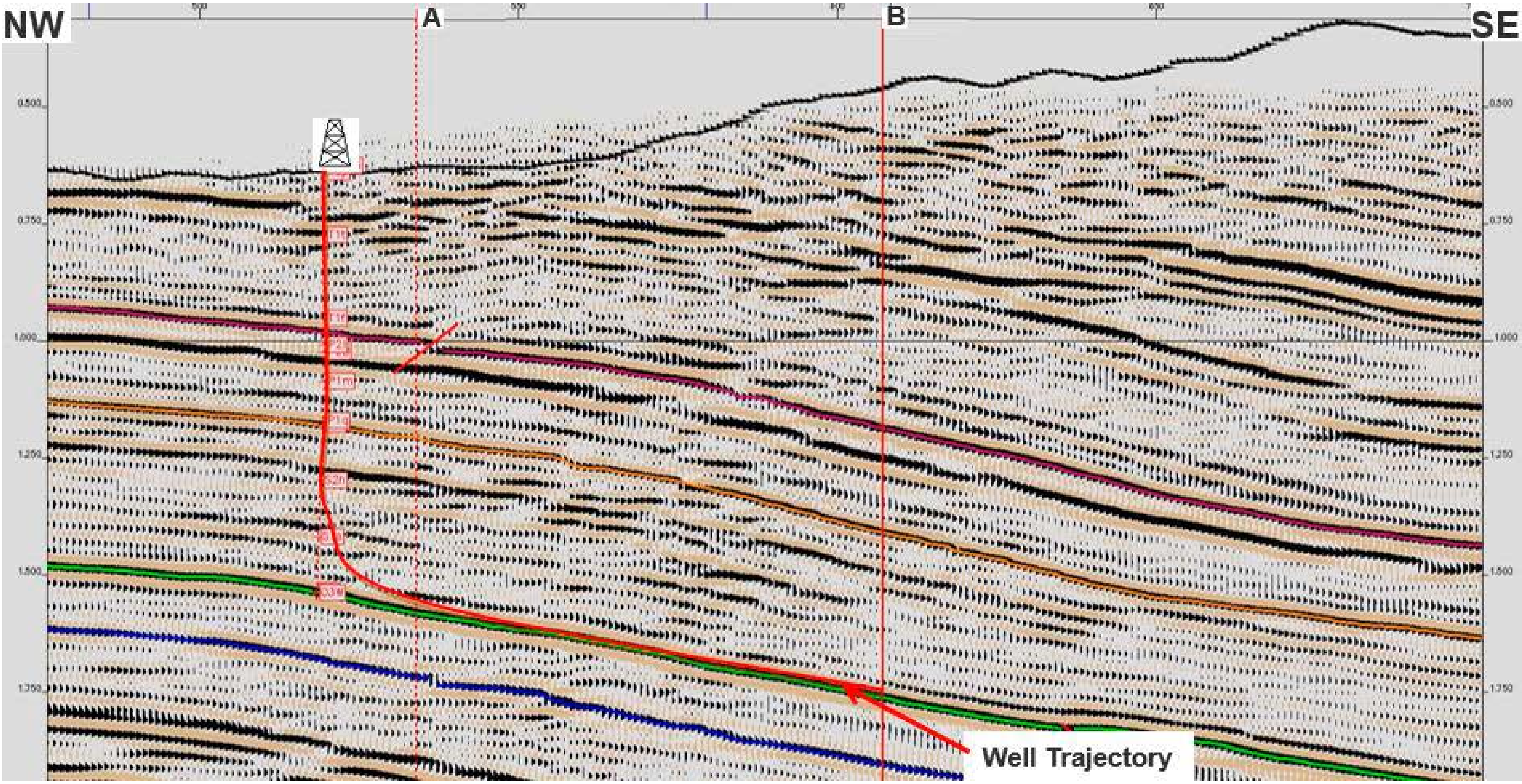

Figure 1. Well trajectory and structure information from surface seismic data.

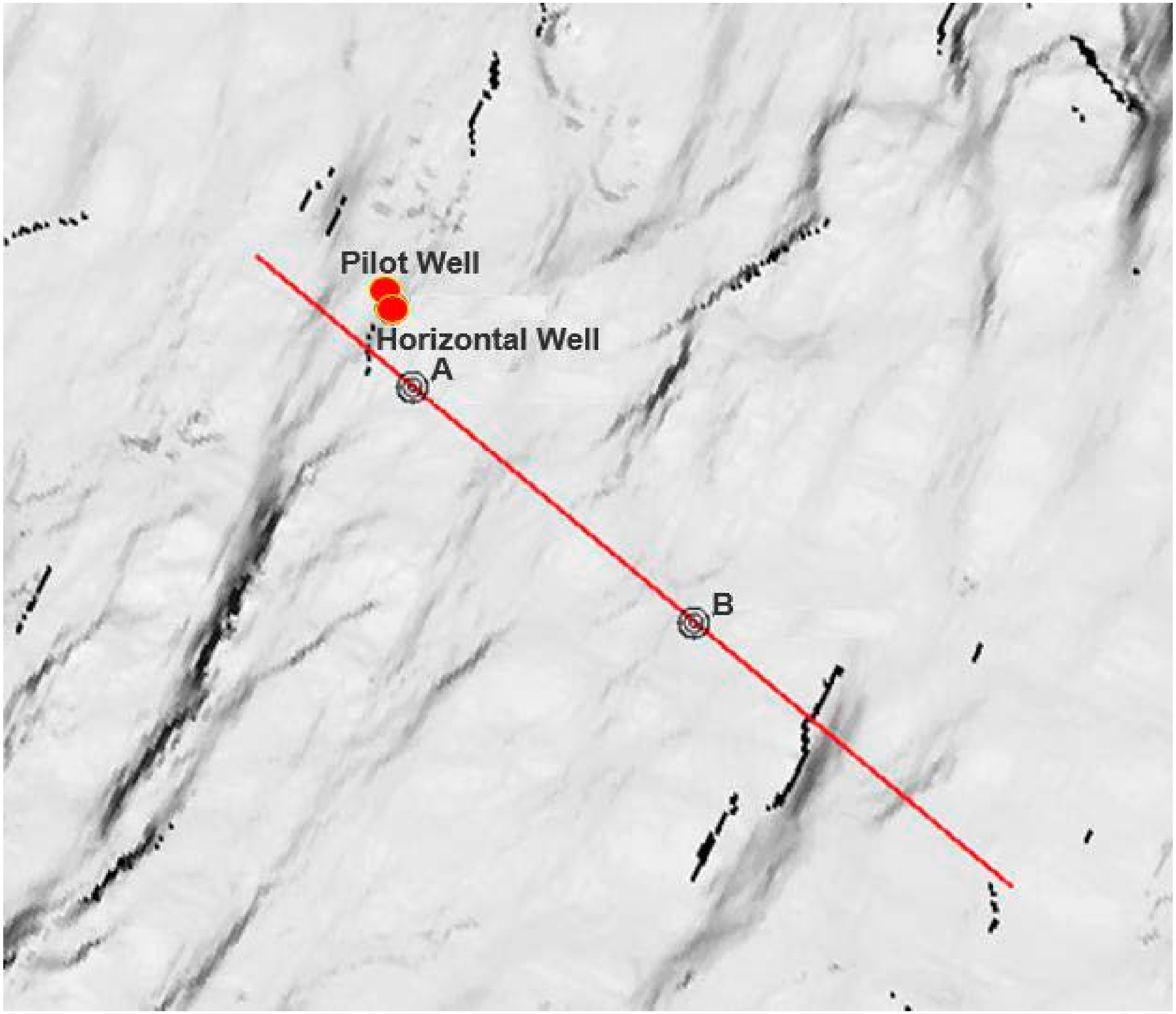

Figure 2. The well trajectory and the faults from an ant-tracking time slice on the bottom of the Ordovician Wufeng Formation underlying the Silurian Longmaxi Formation.

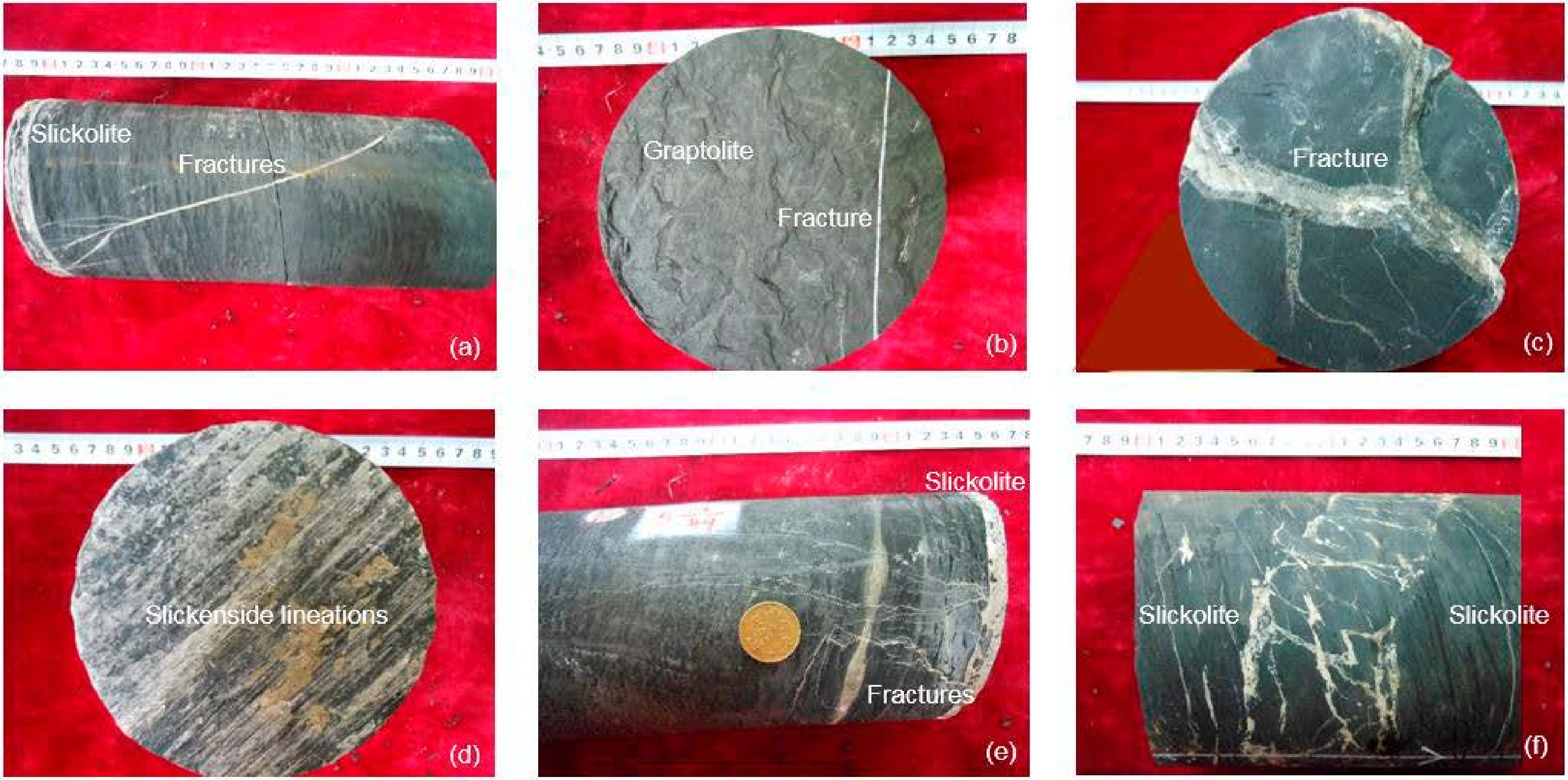

Figure 3. Core photographs showing fractures and slickolites from the pilot well, including high-angle fractures (a), (b), and (c); low-angle shear fracture with slickolite (d); and root-shaped cracks caused by shear slip displacements (e) and (f).

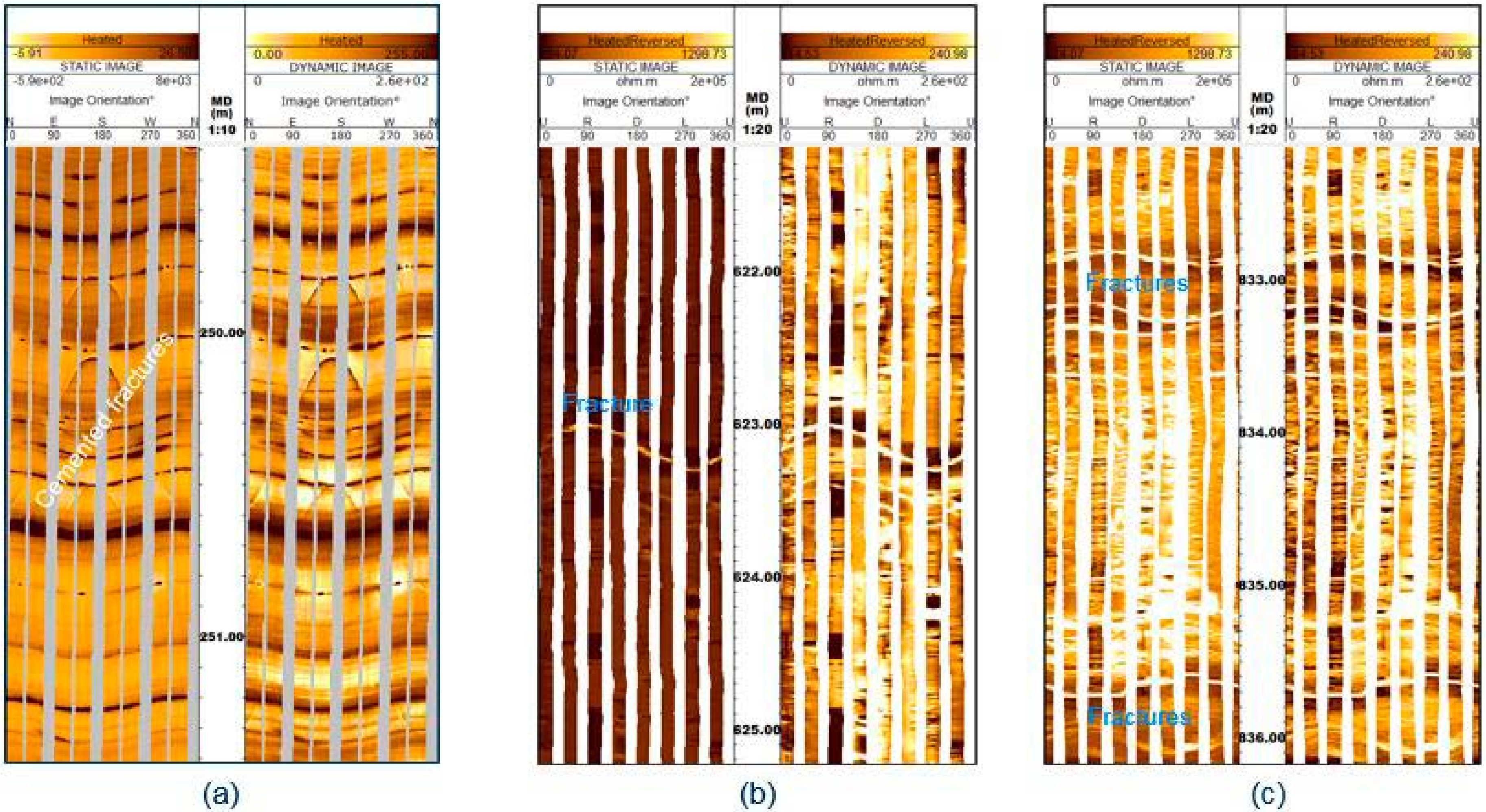

Figure 4. Examples of the fractures (a) on the water-base electrical images from the pilot well in 8.5-in. hole and (b) and (c) on the oil-base microresistivity images from the horizontal section in 8.5-in. hole.

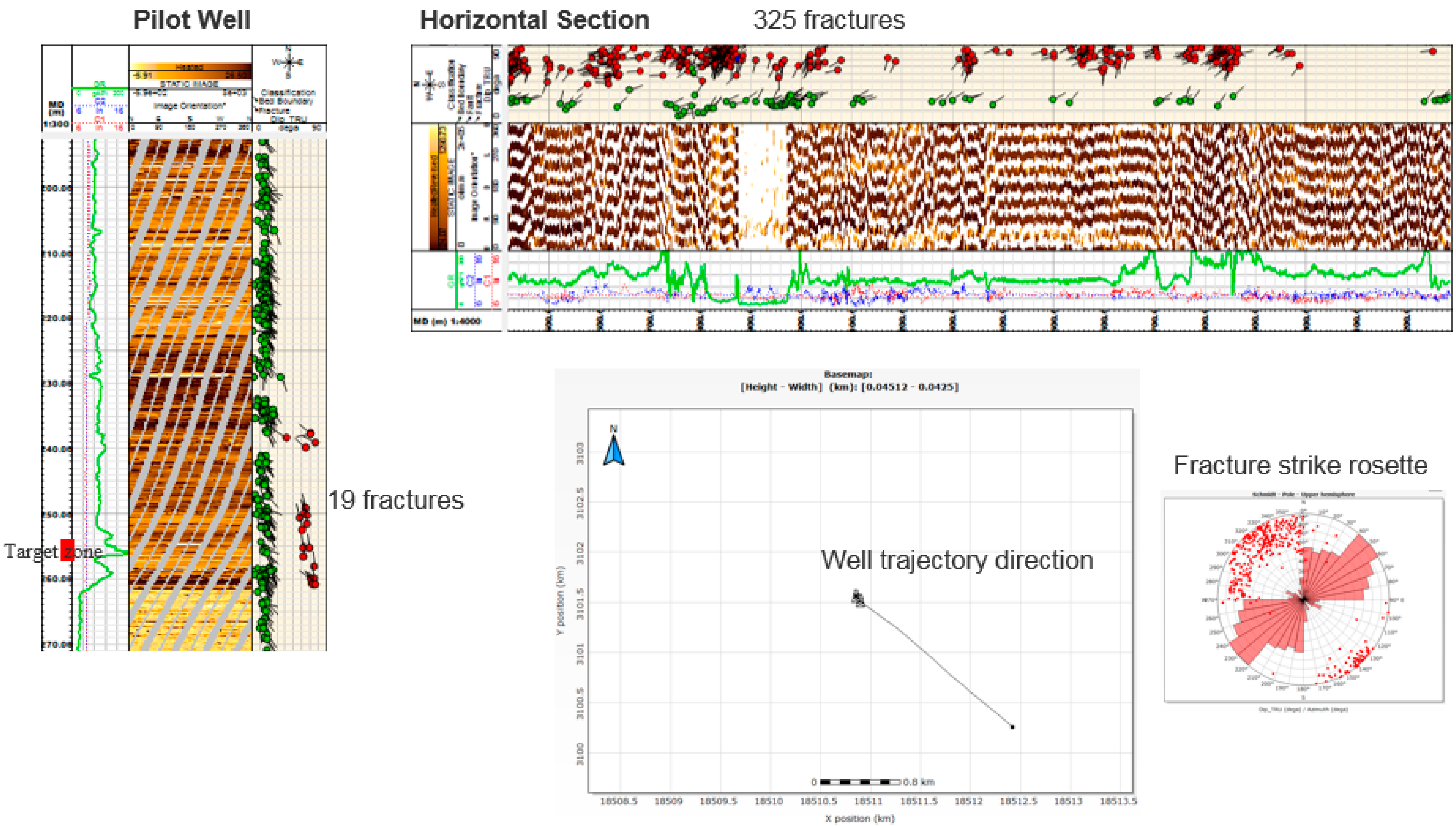

Figure 5. Fracture interpretation from the pilot well and horizontal section, associated with the fracture strike rosette and well trajectory direction. The green tadpole indicates structural dip, and the red tadpole indicates fracture dip.

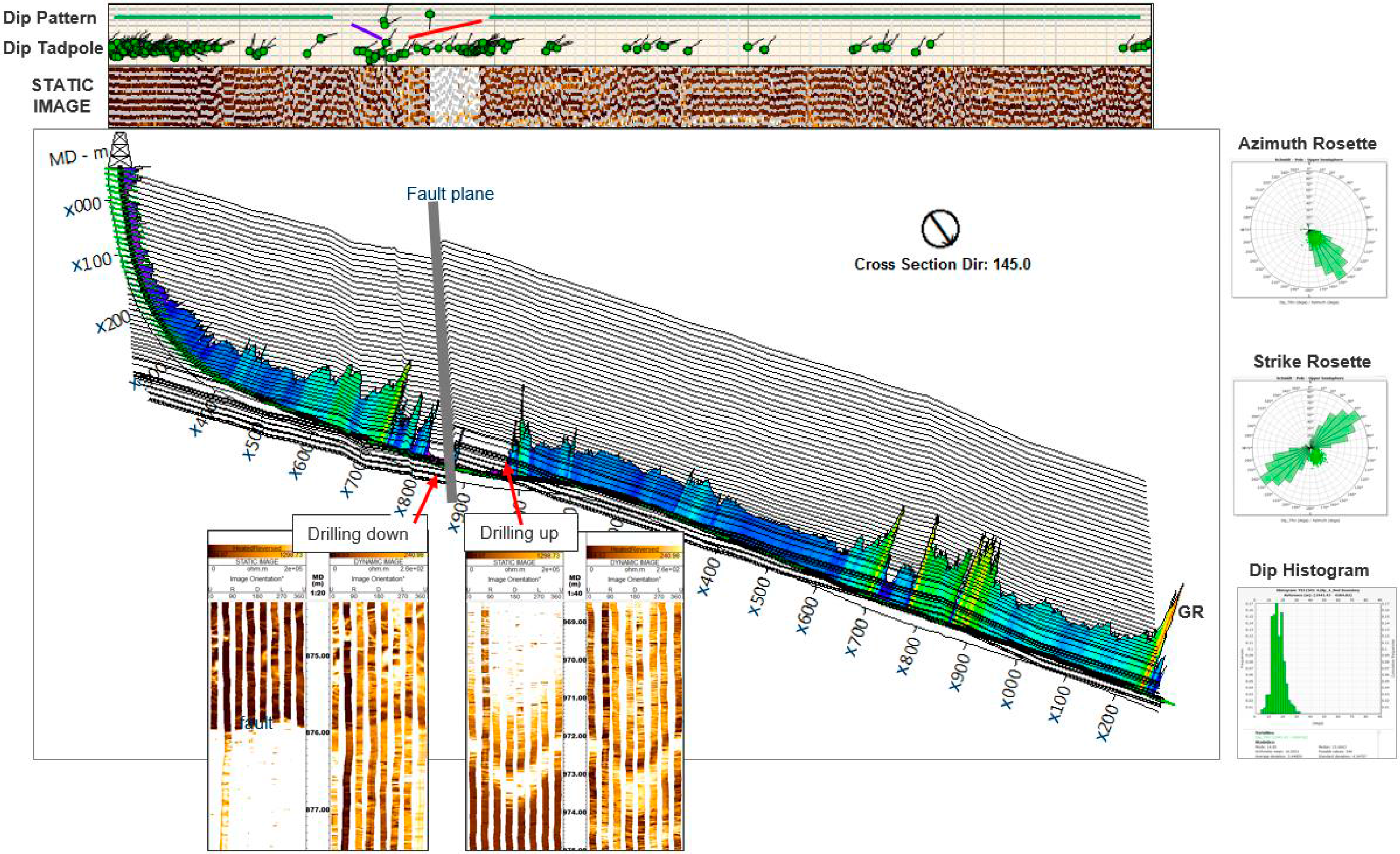

Figure 6. The 2D structure cross section from the interpretation of the oil-base microresistivity image logs, associated with dip patterns, dip tadpoles, static images, structural azimuth rosette, strike rosette, and dip histogram. A main fault occurred at the depth x876 m.

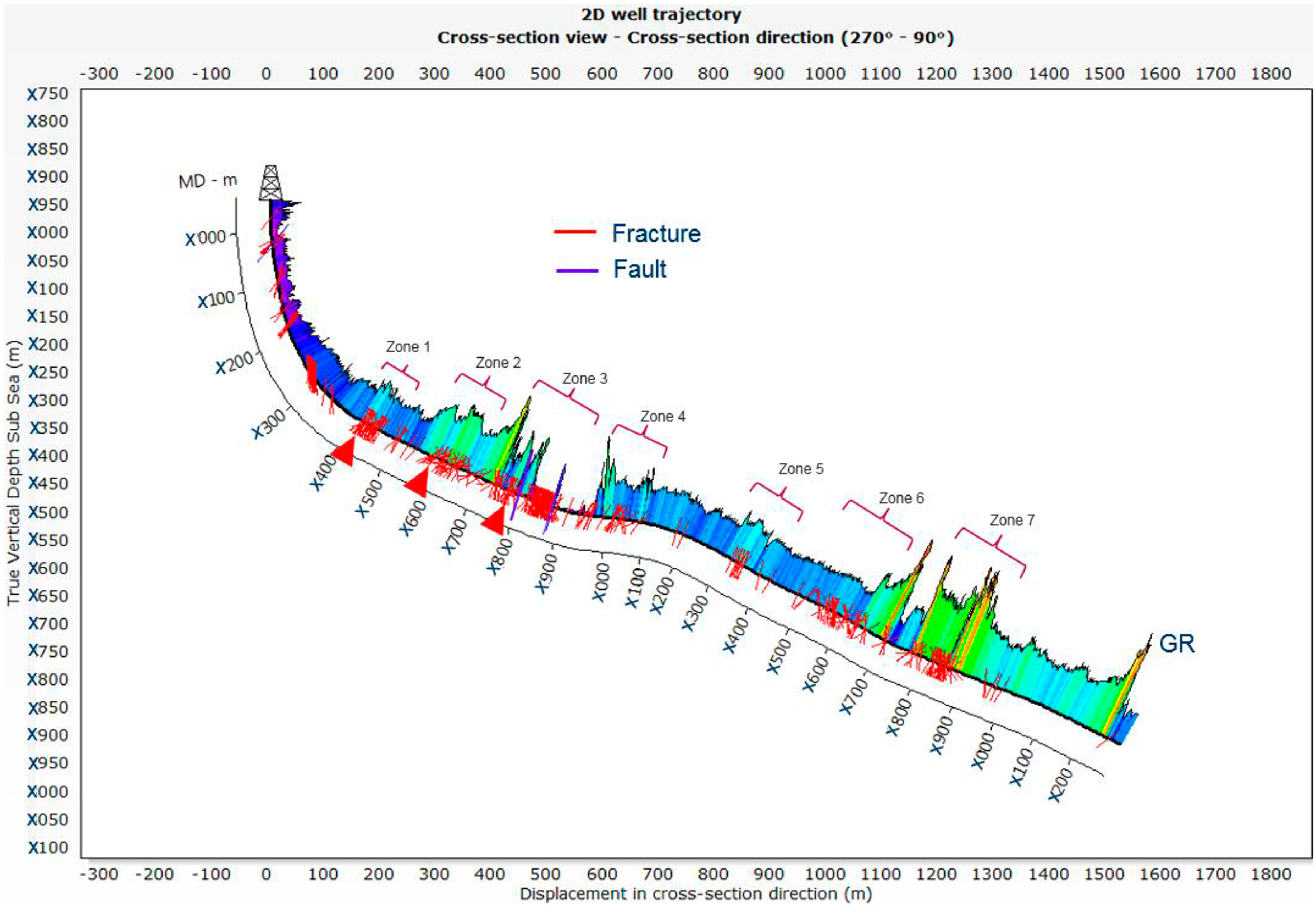

Figure 7. The 2D well trajectory, associated with the gamma ray curve and fractures (red) and fault (blue) stick plot. The red triangles indicate the depths where the mud loss occurred: 37 m3 mud loss at x400 m, 153 m3 mud loss at x596 m, and 93 m3 mud loss at x773 m for a total 342 m3 mud loss in the horizontal section and 28 m3 mud return after stopping pumping for 40 minutes.

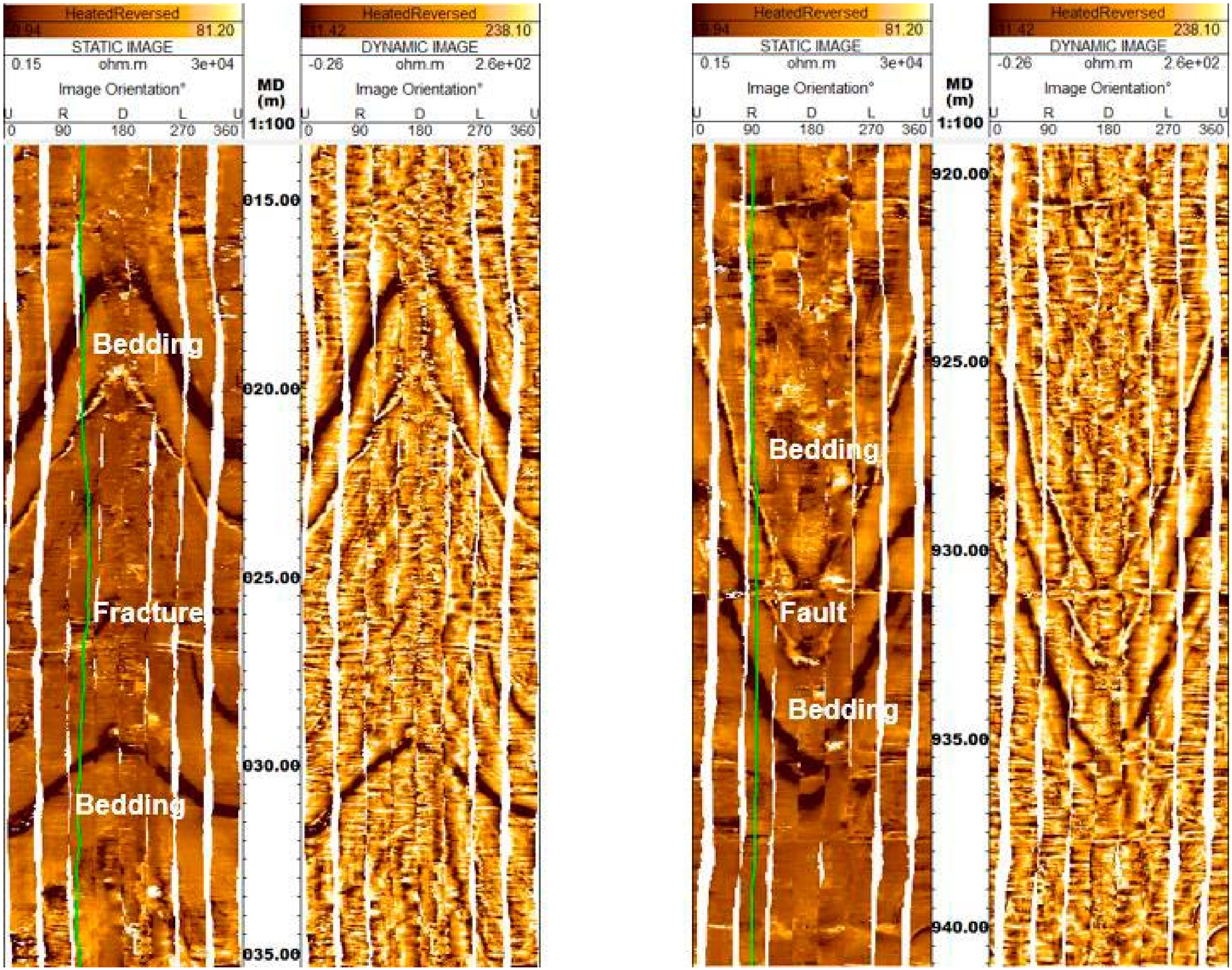

Figure 8. Examples of the new-generation oil-base microresistivity images in the Longmaxi formation from a horizontal well in 8.5-in. hole.